

# A Model for the Enantioselectivity of Imine Reactions Catalyzed by BINOL–Phosphoric Acid Catalysts

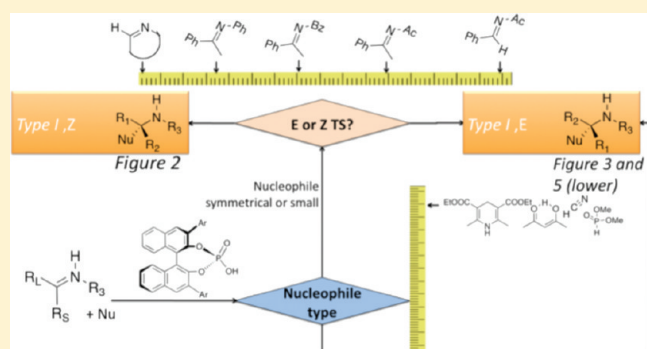
Luis Simón<sup>\*,†</sup> and Jonathan M. Goodman<sup>\*,‡</sup>

<sup>†</sup>Facultad de Ciencias Químicas, Universidad de Salamanca, Plaza de los Caidos 1-5, Salamanca E37004, Spain

<sup>‡</sup>Department of Chemistry, Unilever Centre For Molecular Science Informatics, Lensfield Road, Cambridge CB2 1EW, U.K.

**S** Supporting Information

**ABSTRACT:** BINOL–phosphoric acid catalysts have been used successfully in many reactions involving imines. In this paper, we present a model, based on DFT calculations, for describing the degree and sense of the enantioselectivity of these reactions that is able to predict the correct enantioselectivity for the reactions in more than 40 recent publications. We rationalize the different factors on which the enantioselectivity depends, focusing on the *E*- or *Z*-preference of the transition structures and the orientation of the catalyst with respect to the electrophile.



## INTRODUCTION

The application of BINOL–phosphoric acid catalyst and related compounds has developed very quickly over the past few years.<sup>1–6</sup> We summarize, in the Supporting Information, some of the recent applications of these catalysts. Many of these applications involve the reaction of an imine derivative (*N*-alkyl,<sup>7,8</sup> *N*-aryl,<sup>9–41</sup> *N*-acyl,<sup>42–55</sup> or *N*-tosylimines<sup>56,57</sup>) with a nucleophile that needs to transfer a proton in order to react, such as Hantzsch ester,<sup>9,10,12,13,17,19–22,26–28,35,37,40,48,58–62</sup> benzothiazoline,<sup>11,38</sup> HCN,<sup>7,8</sup> indole,<sup>14,30,49,50,56,57,63</sup> 2- or 3-vinylindoles,<sup>33</sup> phosphites,<sup>24,29,34,41</sup> ketones,<sup>18,36</sup> 1,3-dicarbonyl compounds,<sup>46,64</sup> methanol,<sup>44</sup> peroxides,<sup>53</sup> amides,<sup>31,32</sup>  $\alpha$ -diazoesters,<sup>54</sup> or ene-carbamates.<sup>23,39,43,45,51,52,65</sup> The recently developed SPINOL phosphoric acids also catalyze Friedel–Crafts reactions of indole with *N*-tosyl imines.<sup>66</sup>

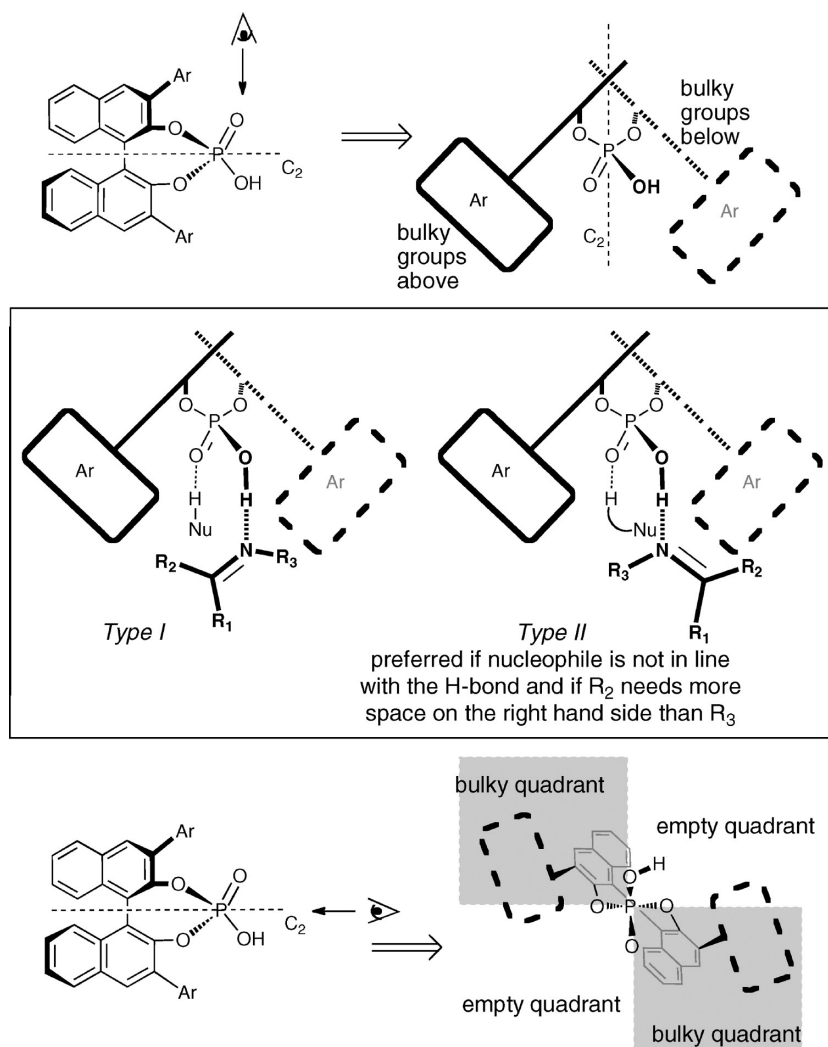
Because of the importance and generality of this catalyst, there have been several different proposals for its mechanism. Akiyama proposed a concerted mechanism for the reaction between *N*-arylimines and phosphite in which the BINOL–phosphoric acid catalyst did not just protonate the imine but also deprotonated the phosphite.<sup>24</sup> Similar mechanisms, in which the BINOL–phosphoric acid catalyst acts simultaneously as an acid and basic catalyst, were proposed for the reactions between indole and *N*-acyl imines,<sup>50</sup> ketones and *N*-aryl imines,<sup>18</sup> or ene-carbamates and *N*-acyl imines.<sup>52</sup> At the same time, stepwise mechanisms were also proposed, in which the acid catalyst first protonates the imine (activating it toward the nucleophilic attack) and is later regenerated by recovering the proton from the protonated nucleophile.<sup>15–17,26</sup>

In our computational study of the Hantzsch ester reduction of *N*-aryl imines, we showed that the concerted mechanism was more likely than the stepwise mechanism, and the stereoselection for the reaction could be explained using a model in which nucleophile and imine were simultaneously attached to the catalyst<sup>67</sup> (in a mechanism similar to that of TBD<sup>68,69</sup> or sulfonic acid<sup>70</sup> catalysis of lactone polymerization). Marcelli and Himo came to similar conclusions, ascribing the catalytic activity of BINOL–phosphoric acid catalyst to Lewis base–Brønsted acid catalysis.<sup>71,72</sup> We have also studied the reaction between HCN and *N*-alkyl imines<sup>73</sup> and between indole and *N*-acyl imines.<sup>74</sup> In both cases, the calculation revealed that the concerted mechanism is more likely than the stepwise mechanism. The reaction between phosphites and *N*-arylimines has been studied independently by Shi,<sup>75</sup> Akiyama,<sup>29</sup> and Yamanaka,<sup>76</sup> and in all these studies the concerted mechanism is also considered the most likely. There is experimental evidence of the interactions between the catalyst and the nucleophile: Zhou observed that BINOL–phosphoric acid catalysts are not effective in the reaction of *N*-alkylated indoles with *N*-acyl imines.<sup>50</sup> Therefore, at least for the reactions of imines with protic nucleophiles, it seems clear that BINOL–phosphoric acid catalysts establish simultaneous interactions with the nucleophile and electrophile.

In our computational studies, we showed that the enantioselectivity of these catalysts is a consequence of the double role of the catalyst. We were able to rationalize this using the classical three-point interaction model<sup>77</sup> that is often employed in

Received: December 7, 2010

Published: February 10, 2011



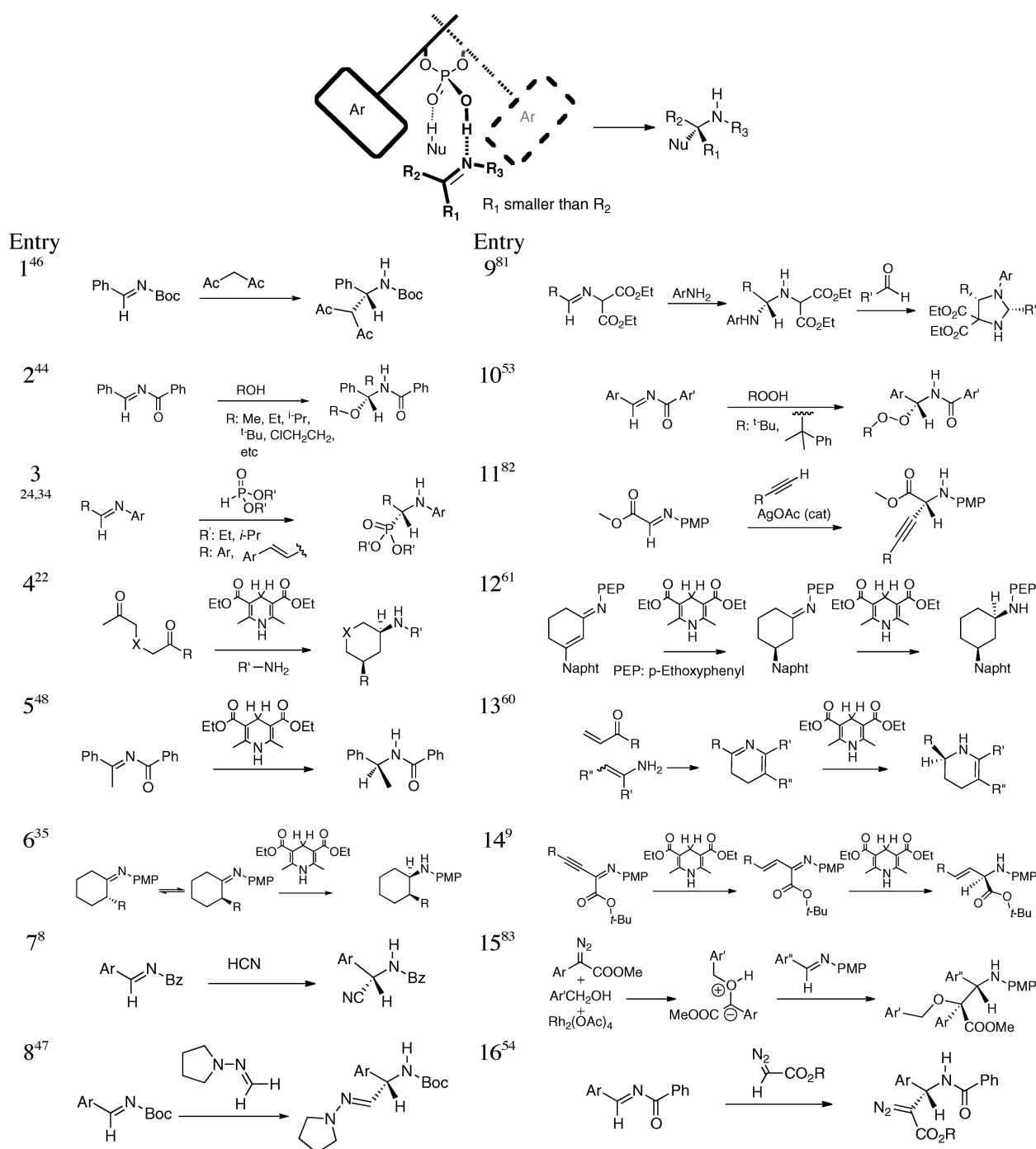
**Figure 1.** Catalyst–imine interactions used in the model proposed to explain the stereoselectivity.<sup>80</sup> The bottom row shows an alternative view of the system that has been used by Himo and Marcelli<sup>71</sup> and Gridnev and Terada.<sup>79</sup>

supramolecular chemistry and chiral recognition.<sup>78</sup> Chiral discrimination between a host and a guest requires the presence of at least three interactions. Chiral induction in a catalytic reaction, which can be explained as chiral discrimination of the catalyst with the two possible enantiomeric transition states, therefore requires at least three different interactions between the catalyst and the reacting complex. Two of these interactions are the H-bonds between the catalyst and the imine and nucleophile. The third is the steric interaction between the bulky substituting groups in the catalyst and groups in the substrate, which favors one of the two possible orientations of the imine H-bonded to the catalyst. In order to predict the sense of the enantioselectivity obtained, we proposed a model based on the projection of the catalyst such that the two BINOL oxygen atoms and the phosphorus atom are in the plane of the paper (Figure 1). Himo and Marcelli<sup>71</sup> and Gridnev and Terada<sup>79</sup> have suggested a different view of the catalytic system, looking down on the system instead of across it, with alternating empty and filled quadrants<sup>71</sup> (Figure 1, bottom). In our projection (Figure 1, top), the free oxygens of the phosphoric acid are above and below the plane of the paper, each having the bulky catalyst substituents on different sides. Deprotonation of the phosphoric

acid gives a  $C_2$ -symmetric structure and so we can arrange the acid catalyst with the OH pointing out of the plane without loss of generality. The imine is drawn at the front and the nucleophile at the back.

For the lowest energy transition structure of reactions with many nucleophiles, the nitrogen substituent of the imine is directed toward the empty side of the oxygen to which it is H-bonded (Figure 1, Type I). The transition structure in which the imine substituent is directed toward the bulky catalyst group (Type II) usually has a higher energy as a consequence of additional steric interactions. This model explains the enantioselectivity obtained for many reactions (Figure 2). These literature results, together with our calculations,<sup>67,73,80</sup> demonstrate the value of the model in predicting the enantioselectivity of nucleophilic addition to imines catalyzed by chiral phosphoric acids.

The stereochemical outcomes of many reactions are explained by the diagram at the top of Figure 2, but there are a few exceptions. Two phenomena can account for these anomalous results: (i) swapping  $R_1$  and  $R_2$  (*E* or *Z*?) and (ii) rotating the imine so the carbon of the double bond is on the right rather than the left as illustrated in Figure 1 (Type I or Type II?).

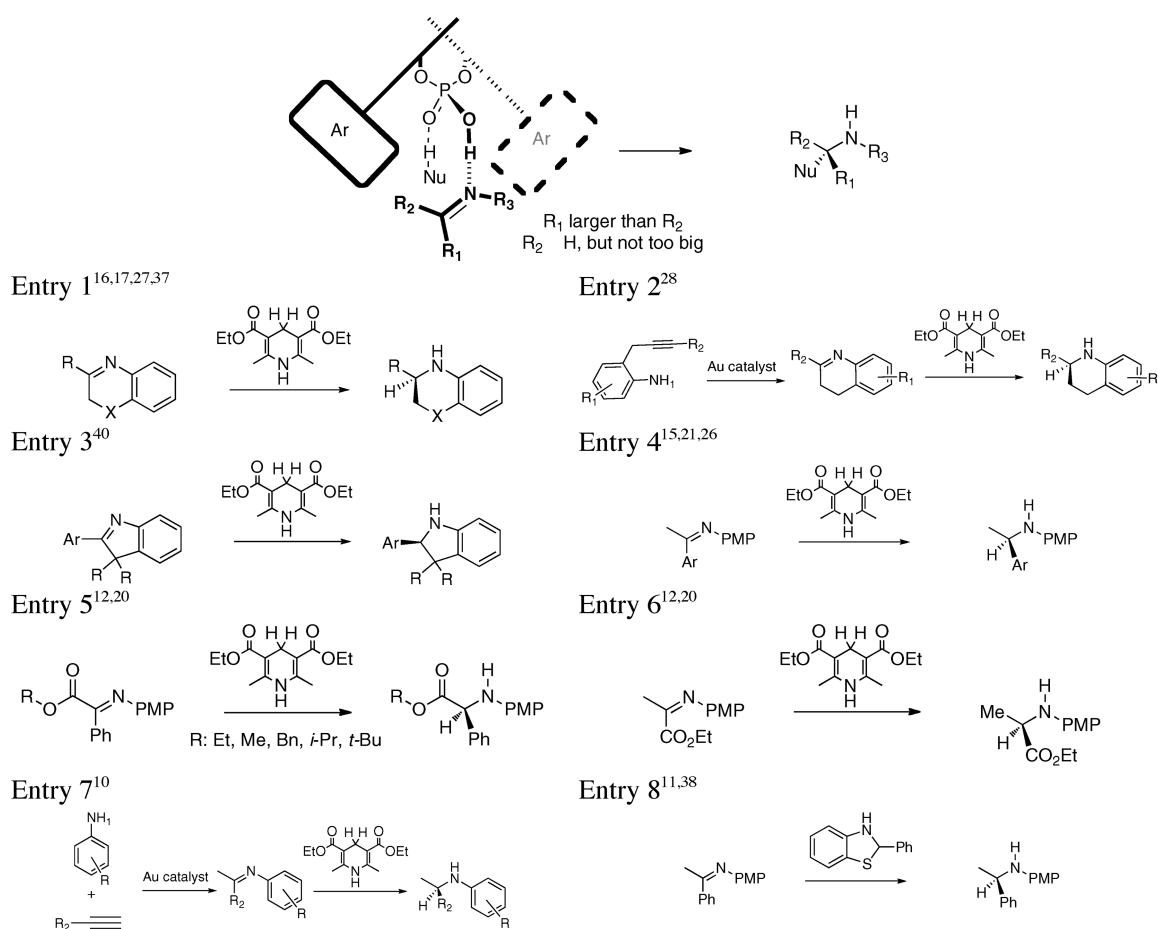


**Figure 2.** Model for the addition reaction of nucleophiles to imines catalyzed by BINOL–phosphoric acid catalyst derivatives (*R* configuration) and its application to some literature reactions (*E* imines and Type I reactions).

## ■ E OR Z DOUBLE BOND?

If  $R_1$  and  $R_2$  are different, the imine geometry affects the stereochemical outcome of the reaction. In Figure 2, the larger group is opposite the protecting group on the imine (usually the *E* configuration). Sometimes, however, the larger group has to be adjacent to the protecting group (usually *Z*): for example, cyclic imines such as quinolines,<sup>16</sup> benzothiazines, benzoxazines, benzoxazinones,<sup>17</sup> quinoxalines, quinoxalinones,<sup>27</sup> and 3H-indoles<sup>40</sup> (Figure 3, left). For the reaction of aldimines (imines derived from aldehydes), the absolute configuration in the product is

consistent with the use of the model in Figure 2 with an *E* imine. For some ketimines (imines derived from ketones), however, the product configuration matches the one observed for cyclic imines (Figure 3, right). This implies that if the model in Figure 2 is used to explain the enantioselectivity, the *N*-phenylimine must react through a *Z* configuration. The energy difference between the *E* and *Z* forms will be smaller for the ketimines than for the aldimines, so this possibility appears to be reasonable. We have confirmed that transition structures originating from *Z* imines lie on the lowest energy pathway in our calculations on the



**Figure 3.** Model for the reaction of addition to phenylketimines. Some examples of literature reactions are given for cyclic imines (entries 1–3) and for phenylketimines (*Z* imines and Type I reactions).

Hantzsch ester reduction of *N*-phenylimines derived from acetophenone<sup>67</sup> and on the addition of HCN to *N*-benzyl imines.<sup>7</sup>

By considering both *E* and *Z* geometries, the model now fits even more of the experimental data. However, problems remain in cases where  $R_1$  is a hydrogen, so the *Z* imine geometry is unlikely, and yet the observed stereochemistry is inverted with respect to our model. In all these cases, the nucleophile is both large and unsymmetrical. Indole is a typical example of such nucleophiles.

### ■ TYPE I OR TYPE II REACTION?

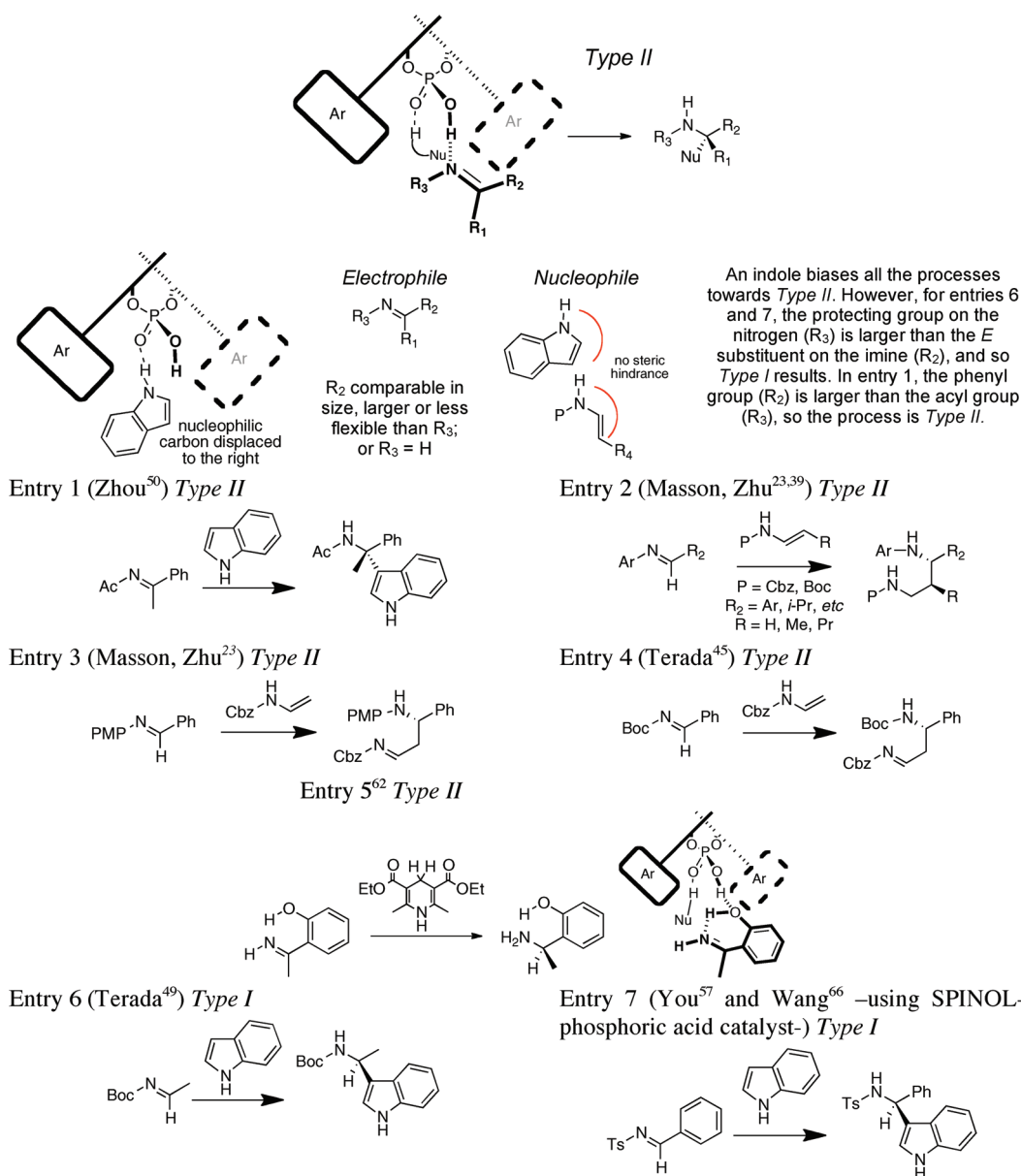
For most of the nucleophiles in Figures 2 and 3, the bond which forms to the electrophile will be directly below the H-bond which holds the nucleophile to the catalyst. For some nucleophiles, however, the new bond may be displaced to one side. Indole is an example of a nucleophile of this type: the benzene ring has to be away from the catalyst, so the nucleophilic carbon is displaced toward it (Figure 4). This can make the imine switch from a Type I to a Type II process, but only if it is reinforced by a large  $R_2$  and a small  $R_3$  group. If the  $R_3$  group is very small (hydrogen), then a Type II process can occur even with a Hantzsch ester nucleophile (Figure 4, entry 5).

In our study<sup>74</sup> of the Friedel–Crafts reaction of indole with *N*-acyl acetophenone ketimine, published by Zhou<sup>50</sup> (Figure 4, entry 1, and Figure 5, top), there were two possible arrangements of the nucleophile with respect to the electrophile (denoted as

endo and exo orientations), and both of these could fit into the catalyst with the imine pointing to the left or to the right. In two of the four possible transition structures (columns 3 and 4 in Figure 5), the indole ring is directed toward the bulky catalyst groups and so the transition structures are too high in energy to be on important reaction pathways. In the remaining two transition structures, endo corresponds to the Type II orientation and exo to the Type I orientation. The most stable transition structure was the Type II (endo).

However, for the reaction of indole with tosylaldimines published by You<sup>57</sup> (Figure 4, entry 7 and Figure 5, bottom), the larger  $R_3$  group reduces the preference for the endo transition structure and increases the negative interactions with the catalyst in a Type II orientation. As a result, the most stable transition structure corresponds to a Type I (exo) structure. The use of SPINOL–phosphoric acid catalyst in this reaction yields the same enantiomer,<sup>66</sup> indicating that the same model probably applies. The addition of indole to *N*-Boc acetaldehyde aldimines (Figure 4, entry 6) published by Terada<sup>49</sup> also gives a product consistent with a Type I (exo) process as the  $R_3$  group (Boc) is also larger than  $R_2$  (methyl).

Masson and Zhu have published an account of the Mannich reaction between *N*-aryldimines and *N*-Cbz- or *N*-Boc-enamines,<sup>39</sup> which is consistent with a Type II mechanism (Figure 4, entry 2). Other reactions for which the enantioselectivity suggests a Type II process are the first step of a Povarov reaction between *N*-Cbz vinyl carbamate and PMP aldimines, which corresponds to the



**Figure 4.** Model for the reaction of Friedel–Crafts reaction of indole and imines catalyzed by BINOL–phosphoric acid derivatives (*E* imines; *Type I* and *Type II* reactions).

addition of the *N*-Cbz vinyl carbamate to the *N*-PMP benzaldehyde aldimine (Figure 4, entry 3) and Terada's cascade reaction between *N*-Boc-aldimines and *N*-Cbz vinyl carbamate<sup>45</sup> (Figure 4, entry 4).

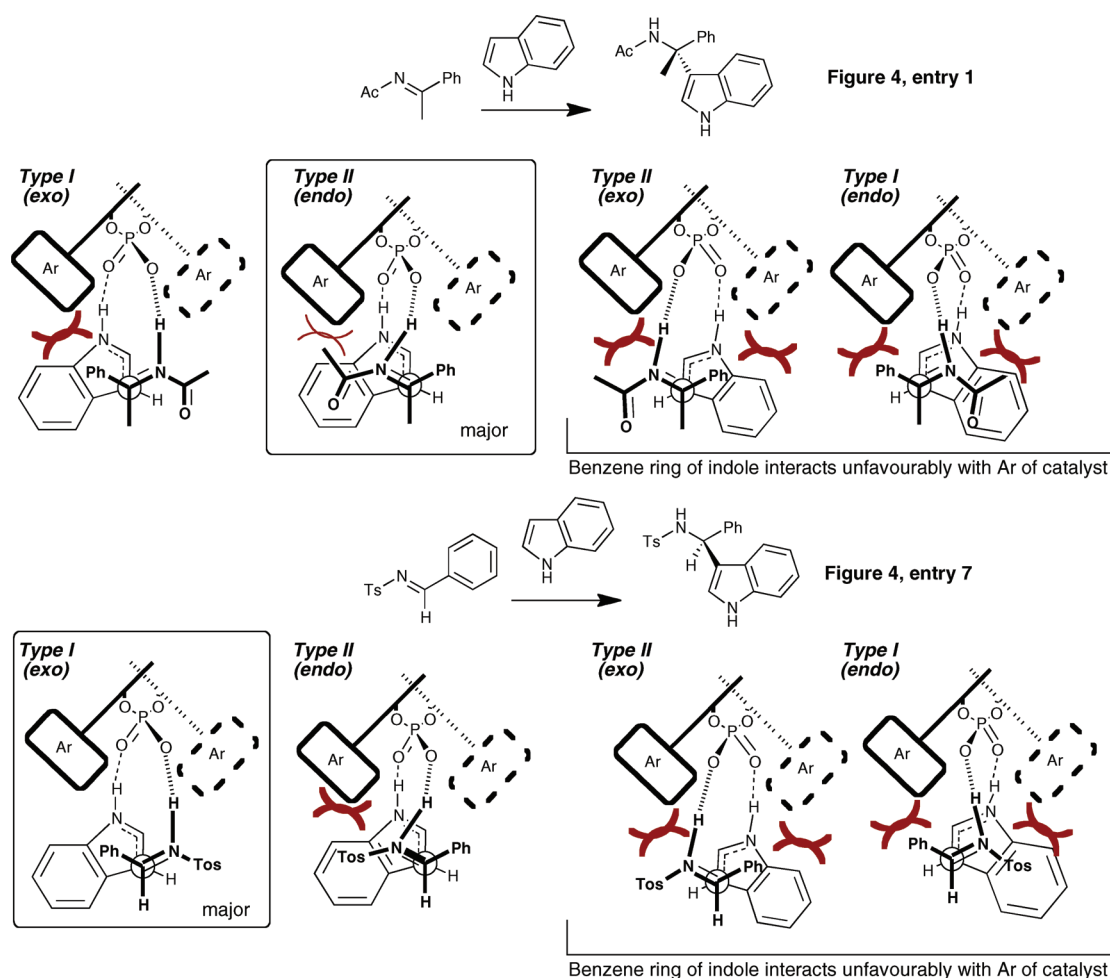
In the Hantzsch ester hydrogenation of *o*-hydroxyarylalkyl ketimines published by Wang<sup>62</sup> (Figure 4, entry 5), the authors propose a model to explain the enantioselectivity based on the Akiyama proposal for the addition of silyl enol ethers to *o*-hydroxy imines catalyzed by BINOL–phosphoric acids.<sup>84</sup> The observed stereochemistry also fits our model provided that the *o*-hydroxy group interacts with the catalyst and that the primary imine prefers a *Type II* model, because its  $R_3$  group (hydrogen) is as small as it possibly can be.

This extensive survey of the literature demonstrates that our model for stereoselectivity fits all the experimental data, once the possibility of *E/Z* isomerism and *Type I* and *Type II* behavior is taken into account. In this paper, we further test our model by

applying it to the Hantzsch ester reduction of *N*-acetylimines and to the reaction of imines with ene–carbamates. The results are investigated using DFT calculations. These are particularly demanding test cases, as two very similar substrates give opposite senses of stereoselection for both (Figures 6 and 10). Together with the literature data gathered in the Supporting Information, this gives us more insights into the factors determining the enantioselectivity of these reactions.

#### ■ HANTZSCH ESTER REDUCTION OF *N*-ACETYLI-MINES: REVERSAL OF STEREOSELECTIVITY BY *E/Z* ISOMERISM

In the recently reported hydrogenation of *N*-acetylimines obtained from enamides<sup>48</sup> (Figure 6), the acetophenone-derived enamide is reduced to the *S* product when the 9-anthryl-substituted *R*-BINOL phosphoric acid is used, and the enantiomeric



**Figure 5.** Models to predict the enantioselectivity in the Friedel–Crafts reaction of indole to acyl (top)<sup>50</sup> ketimines and tosyl<sup>57</sup> (bottom) aldimines.

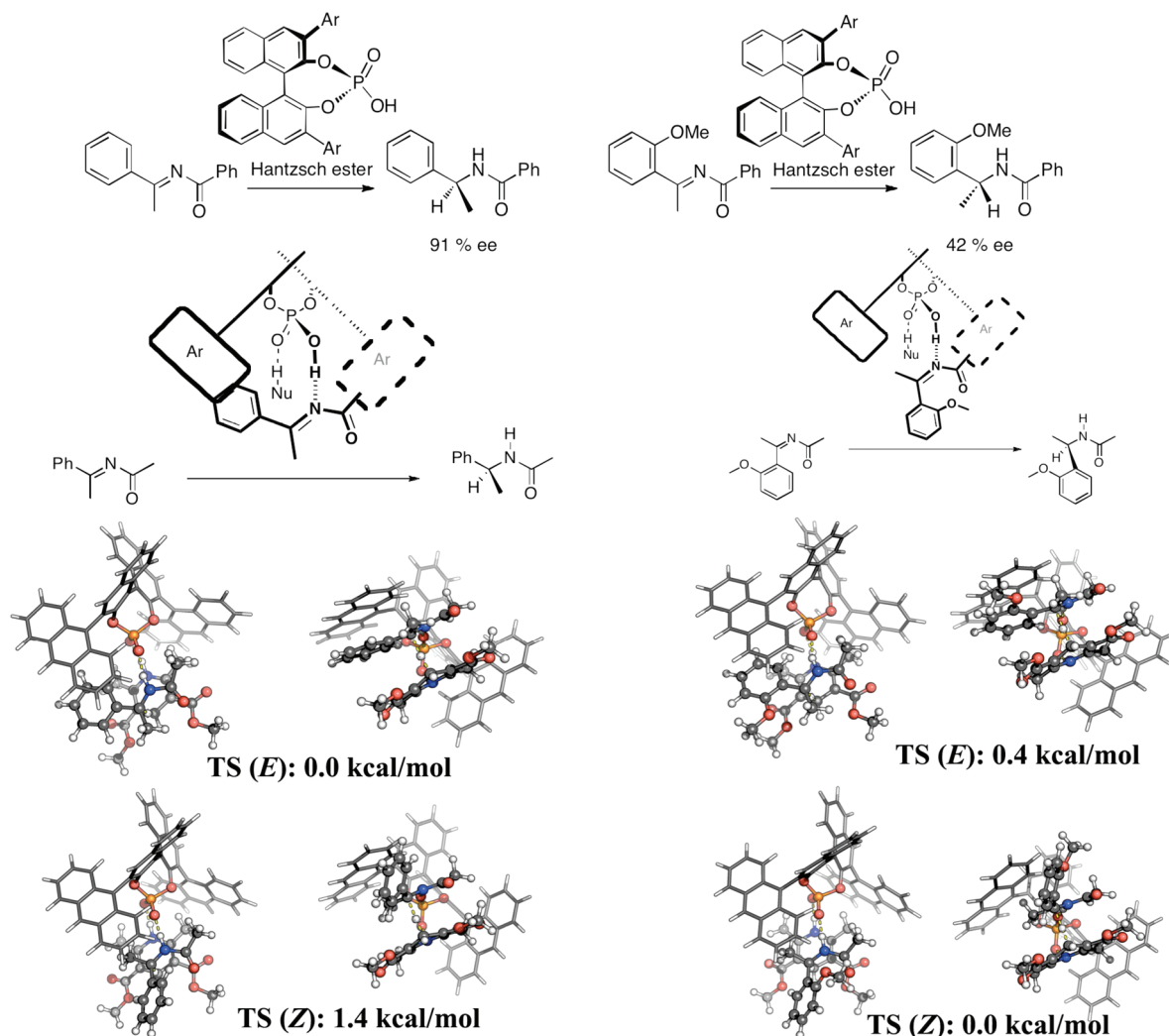
excesses are good (91% ee). However, for the reduction of the (2-methoxyphenyl)methyl ketone derivative, the major product has *R* absolute stereochemistry, and the enantiomeric excess is lower. In order to understand how this small structural modification can lead to this dramatic change in selectivity, we have performed transition structure searches for both substrates. The calculations used the ONIOM hybrid method, with the same level of theory that we employed in our studies of the Hantzsch ester reduction of imines<sup>67</sup> (computational details are available in the Supporting Information).

We considered eight possible transition structures geometries, corresponding to two different conformations for the *N*-acetyl group (*s-cis* or *s-trans*), two different configurations of the imine (*E* and *Z*), and two different orientations of the catalyst, Type I and Type II (Figure 6). For both substrates, the most stable transition structures correspond to Type I. In the reaction of the acetophenone derived imine the *E* transition structure is more stable by 1.4 kcal/mol (83% ee calculated; 91% ee observed). In the reaction of (2-methoxyphenyl)methyl ketone derived imine the *Z* transition structure is 0.4 kcal/mol more stable (27% ee calculated; 41% ee observed). The interaction between the *o*-methoxy group and the imine methyl group twists the aromatic ring out of planarity and so greatly reduces the *E* preference of the ground-state imine. Similar structural features in the transition structures stabilize the *Z* configuration relative to the *E* configuration account for the

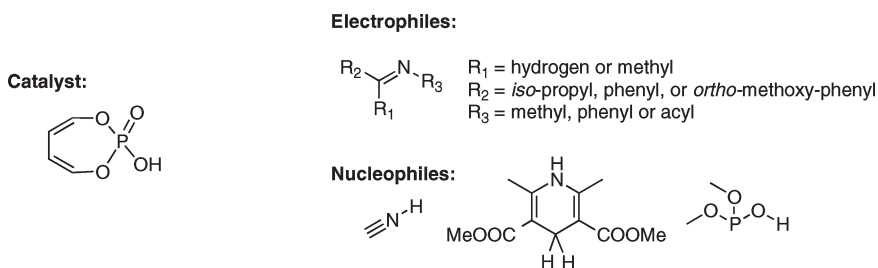
change in the absolute configuration of the product and the reduction of the enantioselectivity.

In order to investigate the factors that determine whether *E* or *Z* imine configuration is preferred in the transition structures, we have performed calculations on three ketimines (acetophenone, 2-methoxyphenyl methyl ketone, and isopropyl methyl ketone) and three aldimines (benzaldehyde, 2-methoxybenzaldehyde, and acetaldehyde). The optimizations were done at the B3LYP/6-31G\*\* level of theory and single-point energy evaluation was done using M05-2X functional; we have recently demonstrated that this is a good level of theory for studying organic reaction mechanisms.<sup>85</sup> Three different nitrogen substitutions were studied: *N*-phenyl, *N*-acetyl, and *N*-methyl. The catalyst was simplified to a buta-1,3-diene-1,4-diol phosphoric acid molecule, which has already been used as a model for the BINOL-phosphoric acid catalyst<sup>67,73</sup> (Figure 7).

For all of the 18 electrophiles in Figure 7, the transition structures for Hantzsch ester reduction, HCN addition and phosphite addition were found. In just one case, the addition of phosphite to *N*-acetylimine derived from acetaldehyde, the transition structure proved elusive. Single-point energy differences between *E* and *Z* transition structures are shown in Table 1; negative values imply that *Z* transition structures are more stable than *E* transition structures. There is a clear preference for *E* configuration in the transition structures for aromatic aldimines, entries 1–9. This is consistent with the results of more complex



**Figure 6.** Antilla's asymmetric reduction of enamides.<sup>48</sup> The figure shows the enantiomeric series to Antilla's results for consistency with the rest of this paper. For the acetophenone-derived imine (left), the TS(*E*) transition state is 1.4 kcal/mol lower in energy than TS(*Z*). An *o*-methoxy group reverses and reduces the ee; TS(*Z*) is now 0.4 kcal/mol lower in energy than TS(*E*).



**Figure 7.** Structures in the study of the relative stability of the *E* and *Z* transition structures.

calculations using the complete catalyst structure for Mannich reactions with a substrate similar to entry 3, and for the Friedel–Crafts reaction of indole with *N*-tosylimines derived from benzaldehyde similar to entry 1. In the case of imines derived from acetaldehyde (entries 7–9), however, this preference is less strong.

In contrast, ketimines often show a preference for *Z* transition structures (Table 1, entries 10–18), even though no imine or iminium shows a strong preference for the *Z* configuration. This is also consistent with earlier calculations, from which we can


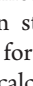
conclude the following: (i) The *Z* configuration is preferred for the Hantzsch ester reduction of *N*-phenyl acetophenone ketimines<sup>67,71</sup> (Table 1, entry 12, and Figure 3, entry 6; Hantzsch ester reduction). (ii) For the Strecker reaction,<sup>73</sup> there is only a small energy difference between competing *E* and *Z* transition structures in the reaction of *N*-benzyl acetophenone ketimines, leading to poor enantioselectivity (consistent with the result in Table 1, entry 11, for the HCN addition). For the reaction of *N*-benzyl benzaldehyde aldimine, the preference for *E* is stronger,

and good enantiomeric excesses are observed (consistent with entry 2). (iii) Despite the *Z* preference of transition structures for *N*-methyl- (entry 11) and *N*-phenylimines (entry 12) derived from acetophenone, the *N*-acetylketimine from acetophenone (entry 10) has a moderate preference for *E* transition structures. As a result, in the Friedel–Crafts addition of indole on *N*-acetylacetophenone ketimine,<sup>74</sup> the lowest energy transition structure has the *E* configuration. The transition structure leading to the minor isomer is very similar, except that it has the *Z* configuration. (iv) The comparison between the Hantzsch ester reduction for entries 10 (good *E* selectivity) and 13 (poor *E/Z* selectivity) shows that the simplified model is able to capture the change in the enantioselectivity for the Antilla reaction (Figure 6).

These four results demonstrate that even this simple model can detect the combinations of ketones and *N* substituents which will lead to small energy differences between *E* and *Z* transition structures. In these cases, poor enantiomeric excesses are expected in the products.

A preference for *Z* transition structures is surprising, particularly as the substrates prefer the *E* configuration. Some of the

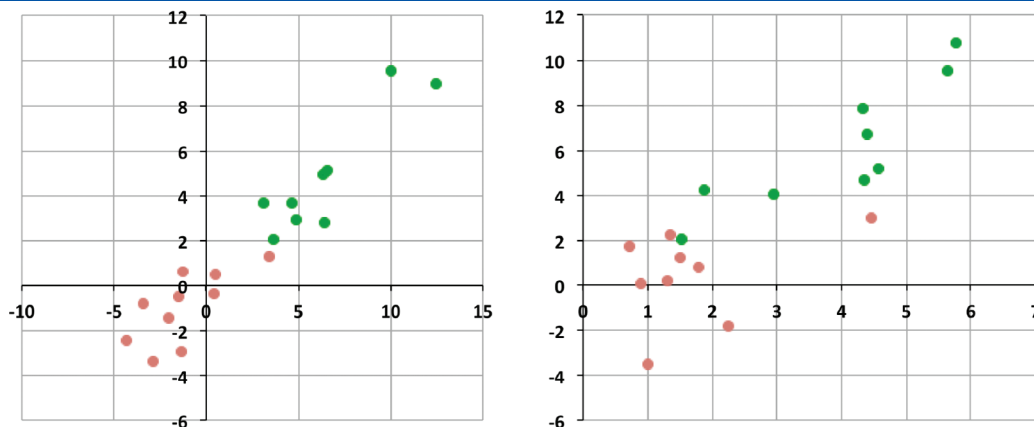
**Table 1. Energy Differences between *E* and *Z* Transition Structures, in kcal/mol (Negative Values Imply That *Z* Structures Are More Stable)**

Entry	Imine			Iminium	HCN	MeOOC	COOMe	MeO	P	O	O	H
	R <sub>1</sub>	R <sub>2</sub>	R <sub>3</sub>									
1	H	Ph	Ac	4.5	7.0	9.5	14.4	8.5				
2	"	"	Me	7.5	1.6	3.7	6.6	5.2				
3	"	"	Ph	5.7	3.0	3.6	7.4	3.0				
4	"		Ac	4.4	6.9	9.0	13.1	6.6				
5	"	"	Me	6.0	2.8	4.9	8.6	6.7				
6	"	"	Ph	5.6	3.0	5.1	11.4	7.0				
7	"	Me	Ac	1.9	4.0	2.8	5.3	—				
8	"	"	Me	1.4	1.6	2.1	2.8	1.3				
9	"	"	Ph	2.3	1.4	2.9	5.8	4.1				
10	Me	Ph	Ac	4.0	4.9	1.3	4.1	3.5				
11	"	"	Me	1.4	1.3	0.6	2.1	4.1				
12	"	"	Ph	2.9	1.6	-2.4	-1.1	-1.9				
13	"		Ac	0.2	3.4	-1.4	0.3	3.5				
14	"	"	Me	0.03	1.4	-0.8	2.2	3.9				
15	"	"	Ph	0.6	1.4	-3.4	-3.8	-3.2				
16	"	<i>iso</i> -Pr	Ac	-0.1	1.9	-0.5	-0.7	1.3				
17	"	"	Ph	1.8	1.2	0.5	0.6	2.7				
18	"	"	Ph	1.2	1.4	-0.04	-0.3	1.2				

factors that favor *E* configuration in the protonated substrates should be partially present in the transition structures, and so for imines obtained from aldehydes, the high energy of *Z* starting materials suggests a high preference for *E* transition structures. In the case of methyl ketone derived imines, the relative stability of *E* transition structures is less, but this does not explain the preference for *Z* transition structures. We performed QRC<sup>86</sup> trajectory calculations from the Strecker reaction transition structures to reactant and product geometries. These structures do not necessarily correspond to the global minima for either the reactants or the products, but to local minimum energy structures located adjacent to the transition structures in the reaction path. We observed a good correlation ( $R^2 = 0.90$ , Figure 8, left) when plotting the energy differences between *E* and *Z* transition structures against the sum of the energy differences in these reactants and products (see the results in the Supporting Information). This indicates that the factors that stabilize a particular configuration in the reactive or product QRC minima are partially present in the transition state structures, which justifies the (sometimes) anomalous preference for a particular configuration.

Considering that transition state search could be a computer-intensive process, obtaining the transition-state structures, even for a simplified model of the catalyst, is not practical. We observed that a plot using the mean of the *E/Z* energy differences for the transition states for all three reactions and the mean of the *E/Z* energy difference of the protonated and unprotonated imines shows also a good correlation ( $R^2 = 0.71$ , Figure 8, right). The mean *E/Z* energy differences can be calculated rapidly and cheaply, as they are simply minimizations of one of the three reactants. This result suggests that aldimine transition structures are always *E* and methyl ketimine transition structures are usually *Z* unless the mean imine/iminium *E* structures are preferred to *Z* by more than 3 kcal/mol.

This analysis requires that the *E/Z* isomerization is faster than the addition reactions. Rotation around a double bond has a substantial energy barrier,<sup>87,88</sup> but the imines are usually generated in situ from a ketone or aldehyde and an amine<sup>14,19,21–23,30,32,38,61,64,81,89–97</sup> by isomerization of the corresponding ene–carbamates to the acyl imine,<sup>48–50</sup> or by activation of a hemiaminal ether.<sup>43</sup> In these cases, if the imine formation is reversible, both *E* and *Z* configurations are accessible.



**Figure 8.** (Left) *E/Z* energy difference in the Strecker reaction transition states plotted against the sum of *E/Z* differences for QRC minima corresponding to products and reactives ( $R^2 = 0.90$ ). (Right) mean TS energy for all three reactions plotted against the mean imine and iminium energy ( $R^2 = 0.71$ ).



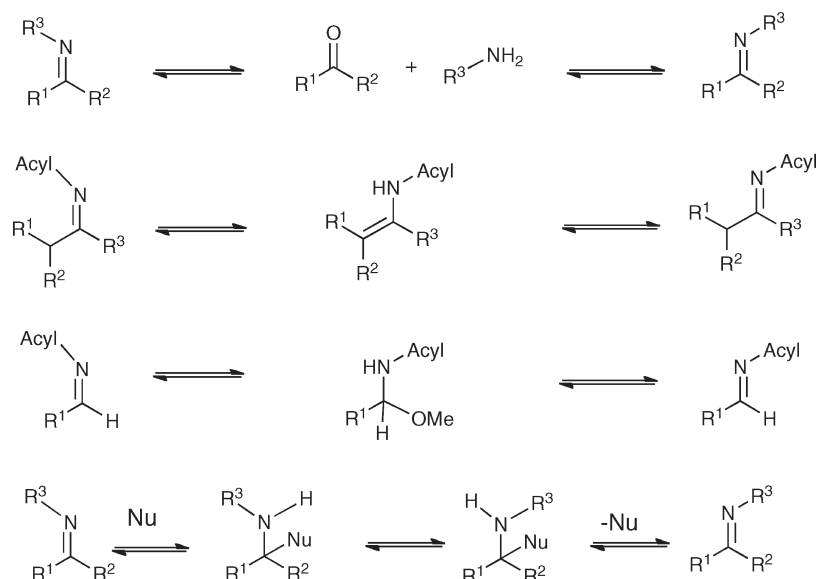


Figure 9. Possible mechanism for the imine *E/Z* isomerization.

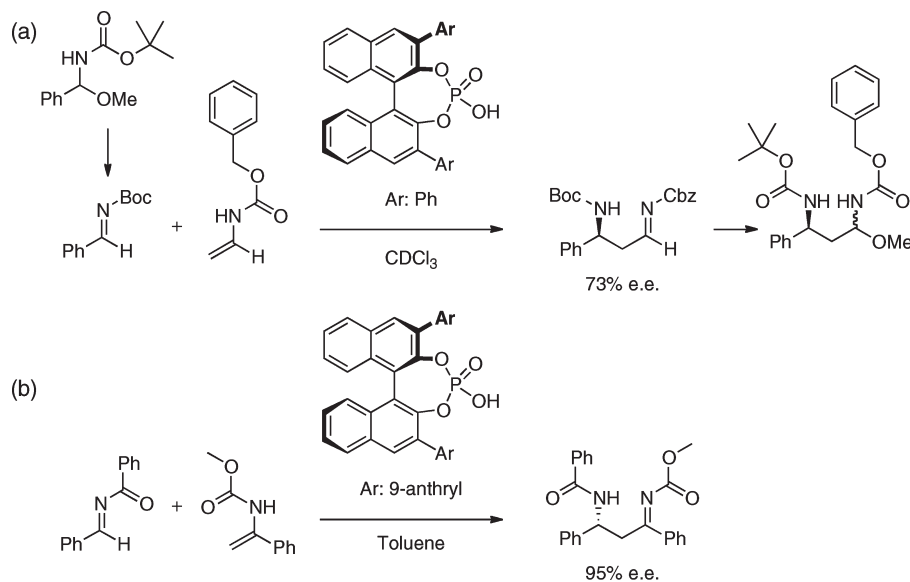


Figure 10. Mannich reactions between acyl imines and vinyl carbamates studied by Terada.<sup>43,52</sup> Despite the similarity of the two processes (a) and (b), the products show opposite stereochemistry.

Another equilibration process is possible at room temperature in the presence of hydroxyl groups,<sup>98,99</sup> through an addition–rotation–elimination mechanism. Other nucleophiles that could also facilitate this process are the amino groups which form in the product of the reaction or else the phosphoric acid catalyst. These possibilities are illustrated in Figure 9.

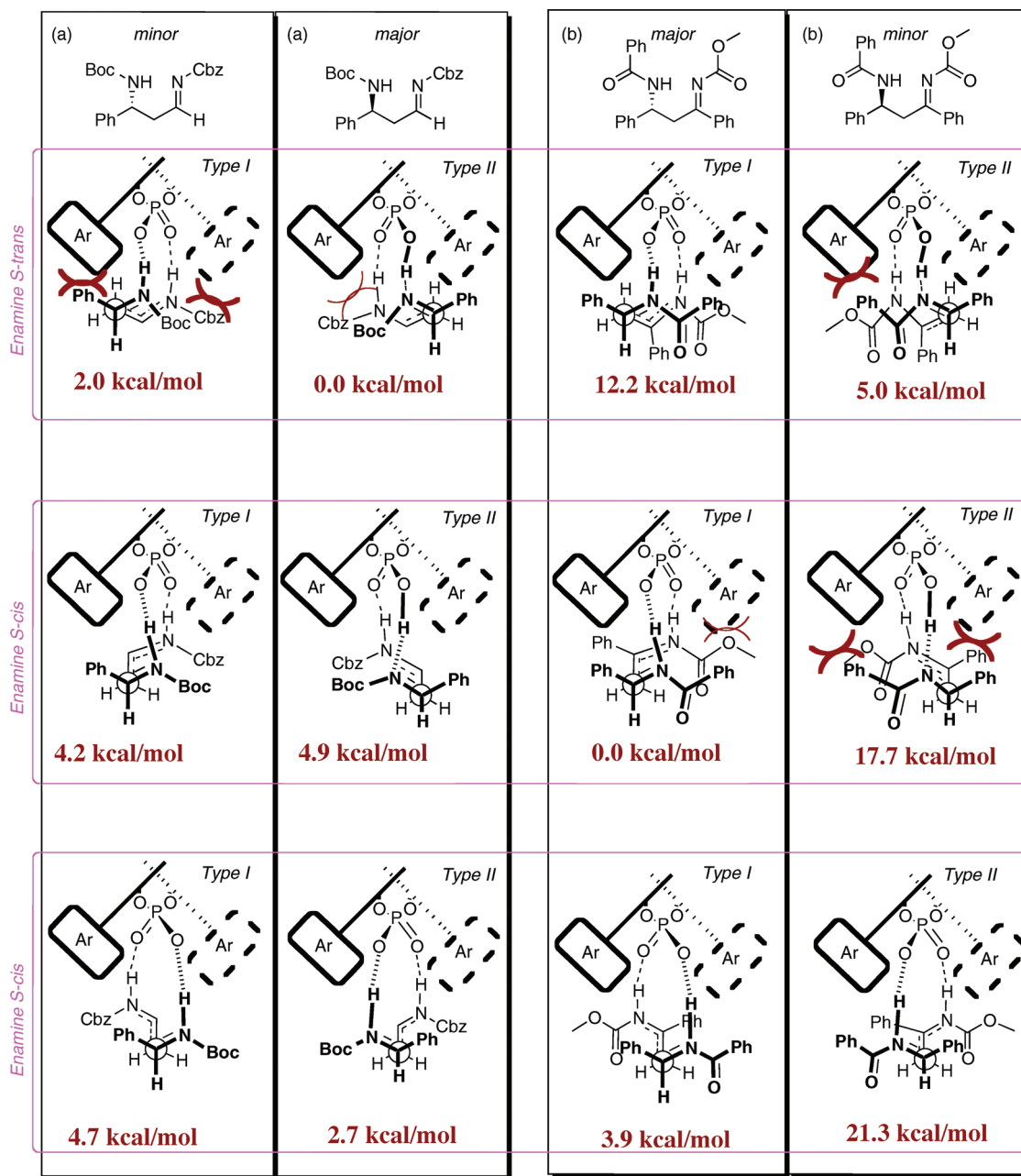
#### ■ TYPE I VS TYPE II PROCESSES: REACTIONS OF ENE–CARBAMATES WITH ACYL IMINES

Terada has published several examples of enantioselective Mannich additions of ene-carbamates to acyl imines catalyzed by BINOL–phosphoric acid derived catalysts.<sup>43,45,52</sup> One interesting result is the reversal in the absolute configuration obtained in the major product of the reaction with 1-phenylvinyl carbamates<sup>52</sup> and vinyl carbamates<sup>43</sup> (Figure 10). This surprising reversal in

stereochemistry should be a good test of models for stereoselectivity in these processes, and so we decided to study the detailed mechanisms of these reactions.

We used the same level of theory as our previous studies of the Hantzsch ester reduction of *N*-acylimines.<sup>67</sup> We considered the different possible conformations of the forming C–C bond that were compatible with the formation of H-bonds between both the nucleophile and electrophile N atoms and the BINOL–phosphoric acid catalyst. Both *E* and *Z* imine configurations were found in the transition structure, but the latter were too high in energy to have any importance for the product and so were not considered further.

Our study of the Friedel–Crafts addition to acyl-imines showed that transition structures with *s-trans* conformation have energy barriers more than 10 kcal/mol higher than the corresponding *s-cis* structures,<sup>74</sup> and so the acyl imines and acyl-enamide



**Figure 11.** Low energy transition structures for the Mannich reactions (a) and (b) from Figure 10. The steric interactions discussed in the text are highlighted.

bonds were given *s-cis* conformation in all the transition structures. In the reaction of *N*-Cbz vinyl carbamate, we also included different rotamers for the benzyl group. The lowest energy transition structures are shown in Figure 11 (higher energy transition structures are listed in the Supporting Information).

The ONIOM calculations show the same reverse in stereoselectivity that is observed experimentally. The lowest energy pathways to the *R* products go through Type I transition structures and the lowest energy pathways to the *S* products go through Type II transition structures.

For reaction (a), Type II transition structures are preferred: the large Cbz group on the nucleophile pushes the sterically undemanding nucleophilic carbon toward the catalyst on the right. For the imine electrophile, the phenyl group ( $R_2$ ) needs the

space on the right-hand side more than the Boc group ( $R_3$ ) that can twist its *tert*-butyl away from the catalyst, and so  $R_2$  is more sterically demanding than  $R_3$ . The corresponding Type I transition structure has a higher energy (2.0 kcal/mol) because the phenyl group of the imine ( $R_2$ ) and the Cbz group of the nucleophile have unfavorable steric interactions with the *R*-BINOL–phosphoric acid substituents. The remaining transition structures correspond to an *s-trans* enamine conformation that is destabilized with respect to the *s-cis* conformation.

For reaction (b), Type I transition structures are preferred. The addition of a phenyl group to the enamine nucleophile leads to a strong preference for an enamine *s-trans* conformation and so destabilizes the reaction (a) preferred transition structure by 5.0 kcal/mol. The reaction (b) phenyl group also destabilizes the

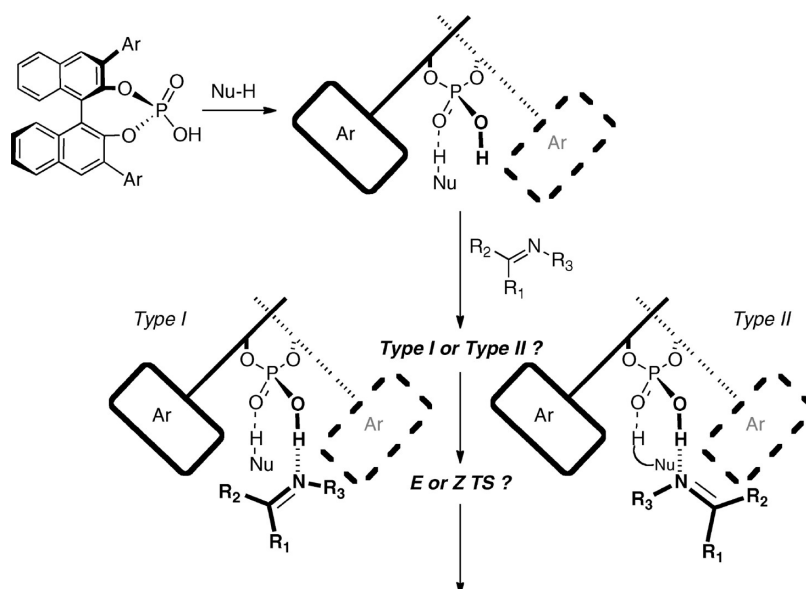


Figure 12. Model for the reaction pathway.

Type II enamine *s-cis* transition structure by 17.7 kcal/mol because the gap between the enamine and the catalyst is large enough for the hydrogen of reaction (a) but much too small for a phenyl group. Rotating the enamine half a turn leads to a Type I geometry, which is the lowest energy transition structure for this reaction. The bad phenyl-catalyst interaction is replaced by the less unfavorable methoxy catalyst interaction. If this methoxy group is replaced by a *tert*-butoxy group, the interaction increases, and the experimentally observed enantioselectivity of the reaction is reduced from 95% ee to 60% ee. A third Type I transition state is also possible, corresponding to the *exo* orientation that we observed in our study of the Friedel–Crafts reaction of indole.<sup>80</sup> This is destabilized by 3.9 kcal/mol probably because in this orientation the nitrogen atoms in the nucleophile and electrophile are too far apart to interact properly with the catalyst.

The stereochemistry of the type II examples in Figure 4 can all be explained by this analysis. Moreover, it can also explain the absolute configuration of the ss chiral centers in the reaction of *N*-aryl aldehyde imines and *N*-Cbz- or *N*-Boc-enamines<sup>39</sup> (Figure 4, entries 2, 3 and 4).

Using all these calculations and experimental results, we suggest a model (Figure 12) to explain the enantioselectivity of the reaction of imines with nucleophiles, catalyzed by BINOL–phosphoric acids.

**a. Type I or Type II.** From the pair of diastereomeric transition structures, the steric interactions with the bulky catalyst substituents can be identified. For the imine, the interactions with the imine N substituent are usually more relevant than the interactions with the C substituents, which favors Type I transition structures; for large and unsymmetrical nucleophiles, their interactions with the catalyst can also be relevant, and this might result in a more stable Type II transition structure. In some cases, such as the enamines, the *s-cis* or *s-trans* conformation of the nucleophile is also important. When the nucleophile adopts the *s-cis* conformation, which must occur for indoles because of their cyclic structure, but also is shown by 1-phenyl enecarbamates, the relative *endo* or *exo* orientation can also affect the stereoselectivity.

**b. E/Z Configuration of the Imine in the Transition Structure.** *Z* transition structure has a higher energy for aldehyde

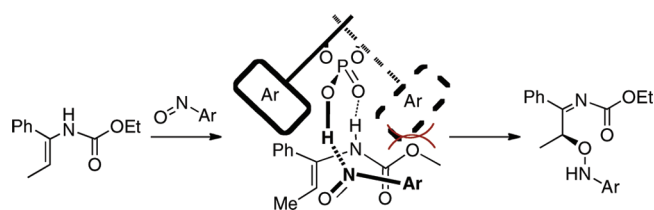


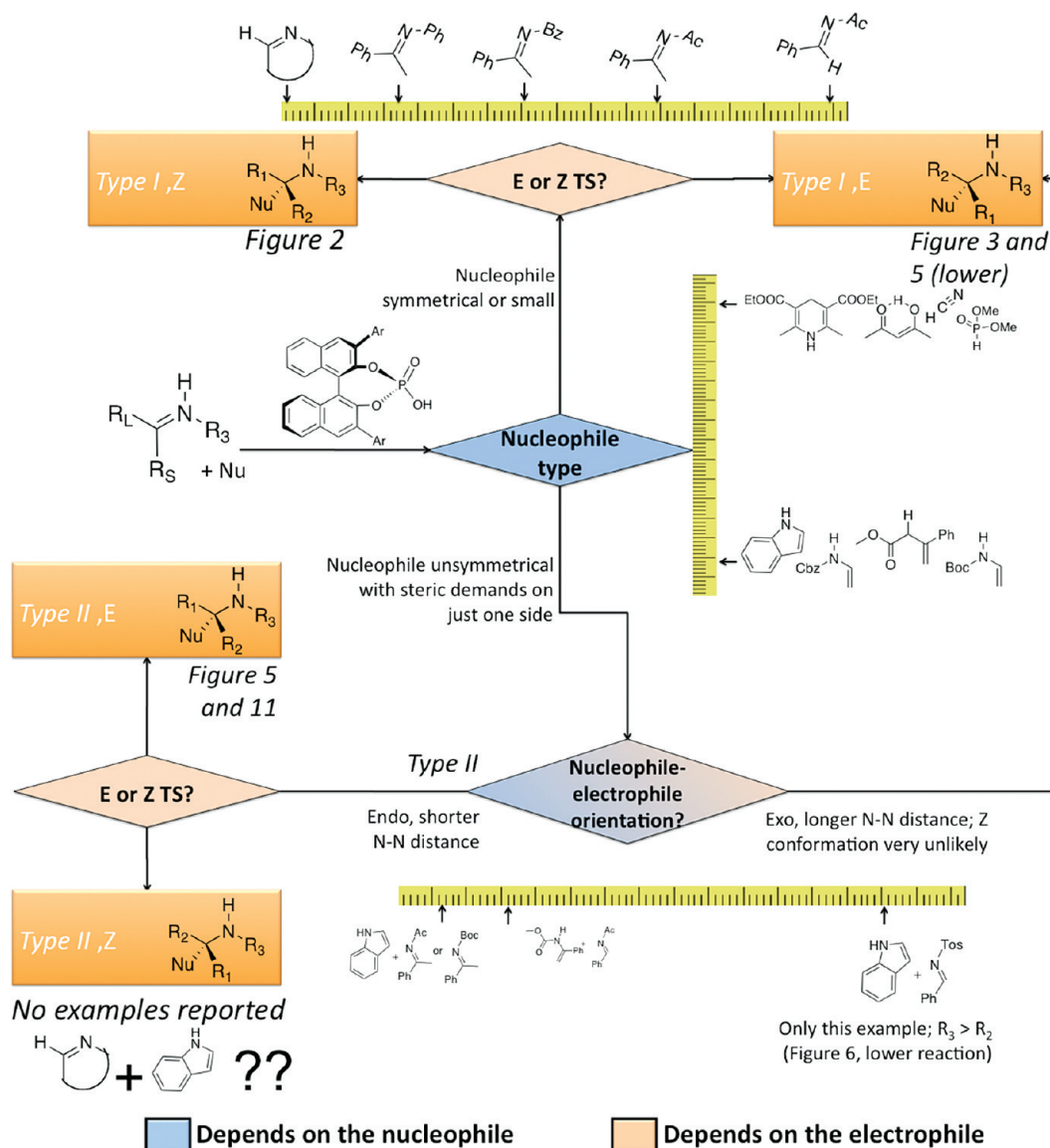
Figure 13. Explanation of the enantioselectivity of the  $\alpha$ -aminoxylation of 1-phenyl propylencarbamate catalyzed by BINOL–phosphoric acids.

imines, but the reaction of ketone imines might not follow this rule. The energy difference for the *E* and *Z* imine ground states can be used to estimate how likely a *Z* transition state may be. An energy difference of less than 3 kcal/mol in favor of *E* in the ground state suggests that a *Z* preference in the transition state is possible.

The same model can be applied to different reactions and to suggest the likely selectivity for  $\beta$ -stereogenic centers as well as  $\alpha$ -centers. The recently published<sup>65</sup>  $\alpha$ -aminoxylation reaction of 1-phenyl propylencarbamate catalyzed by BINOL–phosphoric acid derivatives is another example: unlike in the Mannich reaction, the reaction does not generate a chiral center in the nitroso compound electrophile, but a new chiral center is generated in the ene carbamate depending on its orientation in the transition structure (Figure 13). The most stable conformation of the nucleophile in which the steric interaction between the methyl group and the carbamate carbonyl group is not present, corresponds to the major enantiomer obtained in the reaction.

It is remarkable that these factors can be modified to increase the selectivity of the reaction. For example, for the reaction of 1-phenyl vinyl carbamates, the enantioselectivity will increase if the imine is substituted with smaller groups and more sterically demanding groups are used in the enecarbamate. Conversely, the reaction of nonsubstituted vinyl carbamates will increase the selectivity with larger imine and smaller enecarbamate N-substituents.

The diagram in Figure 14 show how the factors affecting the stereoselectivity can be analyzed to predict the stereochemical outcome of the reactions. Note that for enamine nucleophiles deciding *s-cis* or *s-trans* conformation can also facilitate the prediction of the



**Figure 14.** Summary of the factors that contribute to the structure of the transition structure.

stereochemistry (*s-trans* enamines should always have *endo* relative orientation and react through a *type II* pathway) and allows the configuration of the  $\beta$  center to be established. In order to increase the validity of this diagram with a wider variety of nucleophiles, we have not included the enamine *s-cis/s-trans* possibility. However, in the Supporting Information we include a slightly modified diagram that can be applied for enamines.

## CONCLUSIONS

We have analyzed the enantioselectivity of more than 40 reactions catalyzed by BINOL–phosphoric acid and developed a model which accounts for the stereoselectivity. The model appears to work in all cases and requires analysis only of the transition-state *E/Z* configuration and the choice between Type I and Type II pathways.

We have tested the model by comparing it with a full ONIOM calculation on two reactions for which a small change in the reactants reverses the sense of induction. These are a pair of Hantzsch ester reductions of enamides (Figure 6) and a pair of vinyl carbamate additions (Figure 10). In both cases, the ONIOM calcula-

tions and the qualitative model correctly account for the dramatic effect of a perturbation in the reactants. The first reversal is due to a change from an *E* to a *Z* transition structure. The second is due to a switch from a Type II to a Type I pathway.

The qualitative analysis provides a quick way to select the correct enantiomer of the catalyst to generate a particular product. It also provides guidance about the degree of asymmetric induction. This analysis does not rely on the conformations of the cyclic transition state structures, which could be unpredictable due to the high flexibility of the H-bonds<sup>100–105</sup> involved in the cyclic structures. Instead, configuration of the reactants and their relative orientation to the catalysts are used in the model.

Even though both enantiomers of BINOL–phosphoric acid catalysts are available, the prediction of the absolute configuration of the major enantiomer can still be crucial in a synthetic procedure. Previous material will be wasted if the undesired product is obtained and identification of the product may not be straightforward.<sup>106</sup> The identification of the factors that contribute to the enantioselectivity is important because competing

effects might enhance the overall stereoselectivity, or they could cancel out. We hope that some of these factors are identified in this paper and so can aid the design and analysis of synthetic pathways.

## ■ ASSOCIATED CONTENT

**S Supporting Information.** Summary of recent applications of BINOL–phosphoric acid catalysts. Details of computational methods. Relative energies of *Z* and *E* structures for reactants, products, and QRC minima for the Strecker reaction. Diagram in Figure 14 for enamine nucleophiles. Cartesian coordinates of calculated structures. This material is available free of charge via the Internet at <http://pubs.acs.org>.

## ■ AUTHOR INFORMATION

### Corresponding Author

\*(L.S.) Tel: +34 (0) 923 294482. Fax: +34 (0)923 294514. E-mail: [lsimon@usal.es](mailto:lsimon@usal.es). (J.M.G.) Tel: +44 (0)1223 336434. Fax: +44 (0)1223 763076. E-mail: [jmg11@cam.ac.uk](mailto:jmg11@cam.ac.uk).

## ■ ACKNOWLEDGMENT

This research was supported by a Marie Curie Intra-European Fellowship within the 6th European Community Framework Programme MEIF-CT2006-040554 and a Marie-Curie Reintegration Grant within the 7th European Community Framework Programme PERG04-GA-2008-239244. We acknowledge the use of CamGrid service in carrying out this work.

## ■ REFERENCES

- Terada, M. *Chem. Commun.* **2008**, 4097.
- Akiyama, T. *Chem. Rev. (Washington, DC)* **2007**, *107*, 5744.
- Dalko, P. I. *Enantioselective Organocatalysis, Reactions and Experimental Procedures*; Wiley-VCH: Weinheim, 2007.
- Zamfir, A.; Schenker, S.; Freund, M.; Tsogoeva, S. B. *Org. Biomol. Chem.* **2010**, *8*, 5262.
- Albrecht, L. u.; Albrecht, A.; Krawczyk, H.; Jørgensen, K. A. *Chem.—Eur. J.* **2010**, *16*, 24.
- Kampen, D.; Reisinger, C. M.; List, B. In *Topics in Current Chemistry*; List, B., Ed.; Springer-Verlag: Berlin, 2009; Vol. 291, p 395.
- Rueping, M.; Sugiono, E.; Moreth, S. A. *Adv. Synth. Catal.* **2007**, *349*, 759.
- Rueping, M.; Sugiono, E.; Azap, C. *Angew. Chem., Int. Ed.* **2006**, *45*, 2617.
- Kang, Q.; Zhao, Z.-A.; You, S.-L. *Org. Lett.* **2008**, *10*, 2031.
- Liu, X.-Y.; Che, C.-M. *Org. Lett.* **2009**, *11*, 4204.
- Zhu, C.; Akiyama, T. *Org. Lett.* **2009**, *11*, 4180.
- Kang, Q.; Zhao, Z.-A.; You, S.-L. *Adv. Synth. Catal.* **2007**, *349*, 1657.
- Rueping, M.; Theissmann, T.; Raja, S.; Bats, J. W. *Adv. Synth. Catal.* **2008**, *350*, 1001.
- Zhang, G.-W.; Wang, L.; Nie, J.; Ma, J.-A. *Adv. Synth. Catal.* **2008**, *350*, 1457.
- Hoffmann, S.; Seayad, A. M.; List, B. *Angew. Chem., Int. Ed.* **2005**, *44*, 7424.
- Rueping, M.; Antonchick, A. P.; Theissmann, T. *Angew. Chem., Int. Ed.* **2006**, *45*, 3683.
- Rueping, M.; Antonchick, A. P.; Theissmann, T. *Angew. Chem., Int. Ed.* **2006**, *45*, 6751.
- Guo, Q.-X.; Liu, H.; Guo, C.; Luo, S.-W.; Gu, Y.; Gong, L.-Z. *J. Am. Chem. Soc.* **2007**, *129*, 3790.
- Hoffmann, S.; Nicoletti, M.; List, B. *J. Am. Chem. Soc.* **2006**, *128*, 13074.
- Li, G.; Liang, Y.; Antilla, J. C. *J. Am. Chem. Soc.* **2007**, *129*, 5830.
- Storer, R. I.; Carrera, D. E.; Ni, Y.; MacMillan, D. W. C. *J. Am. Chem. Soc.* **2006**, *128*, 84.
- Zhou, J.; List, B. *J. Am. Chem. Soc.* **2007**, *129*, 7498.
- Liu, H.; Dagousset, G.; Masson, G.; Retaillieu, P.; Zhu, J. *J. Am. Chem. Soc.* **2009**, *131*, 4598.
- Akiyama, T.; Morita, H.; Itoh, J.; Fuchibe, K. *Org. Lett.* **2005**, *7*, 2583.
- Liu, H.; Cun, L.-F.; Mi, A.-Q.; Jiang, Y.-Z.; Gong, L.-Z. *Org. Lett.* **2006**, *8*, 6023.
- Rueping, M.; Sugiono, E.; Azap, C.; Theissmann, T.; Bolte, M. *Org. Lett.* **2005**, *7*, 3781.
- Rueping, M.; Tato, F.; Schoepke, F. R. *Chem.—Eur. J.* **2010**, *16*, 2688.
- Han, Z.-Y.; Xiao, H.; Chen, X.-H.; Gong, L.-Z. *J. Am. Chem. Soc.* **2009**, *131*, 9182.
- Akiyama, T.; Morita, H.; Bachu, P.; Mori, K.; Yamanaka, M.; Hirata, T. *Tetrahedron* **2009**, *65*, 4950.
- Kang, Q.; Zhao, Z.-A.; You, S.-L. *Tetrahedron* **2009**, *65*, 1603.
- Rueping, M.; Antonchick, A. P.; Sugiono, E.; Grenader, K. *Angew. Chem., Int. Ed.* **2008**, *48*, 908.
- Cheng, X.; Vellalath, S.; Goddard, R.; List, B. *J. Am. Chem. Soc.* **2008**, *130*, 15786.
- Bergonzini, G.; Gramigna, L.; Mazzanti, A.; Fochi, M.; Bernardi, L.; Ricci, A. *Chem. Commun.* **2010**, *46*, 327.
- Bhadury, P. S.; Zhang, Y.; Zhang, S.; Song, B.; Yang, S.; Hu, D.; Chen, Z.; Xue, W.; Jin, L. *Chirality* **2009**, *21*, 547.
- Wakchaure, V. N.; Zhou, J.; Hoffmann, S.; List, B. *Angew. Chem., Int. Ed.* **2010**, *49*, 4612.
- Rueping, M.; Sugiono, E.; Schoepke, F. R. *Synlett* **2007**, 1441.
- Metallinos, C.; Barrett, F. B.; Xu, S. *Synlett* **2008**, 720.
- Enders, D.; Liebich, J. X.; Raabe, G. *Chem.—Eur. J.* **2010**, *16*, 9763.
- Dagousset, G.; Drouet, F.; Masson, G.; Zhu, J. *Org. Lett.* **2009**, *11*, 5546.
- Rueping, M.; Brinkmann, C.; Antonchick, A. P.; Atodiresei, I. *Org. Lett.* **2010**, *12*, 4604.
- Xu, W.; Zhang, S.; Yang, S.; Jin, L.-H.; Bhadury, P. S.; Hu, D.-Y.; Zhang, Y. *Molecules* **2010**, *15*, 5782.
- Terada, M.; Yokoyama, S.; Sorimachi, K.; Uruguchi, D. *Adv. Synth. Catal.* **2007**, *349*, 1863.
- Terada, M.; Machioka, K.; Sorimachi, K. *Angew. Chem., Int. Ed.* **2009**, *48*, 2553.
- Li, G.; Fronczek, F. R.; Antilla, J. C. *J. Am. Chem. Soc.* **2008**, *130*, 12216.
- Terada, M.; Machioka, K.; Sorimachi, K. *J. Am. Chem. Soc.* **2007**, *129*, 10336.
- Uruguchi, D.; Terada, M. *J. Am. Chem. Soc.* **2004**, *126*, 5356.
- Rueping, M.; Sugiono, E.; Theissmann, T.; Kuenkel, A.; Kockritz, A.; Pews-Davtyan, A.; Nemati, N.; Beller, M. *Org. Lett.* **2007**, *9*, 1065.
- Li, G.; Antilla, J. C. *Org. Lett.* **2009**, *11*, 1075.
- Terada, M.; Sorimachi, K. *J. Am. Chem. Soc.* **2007**, *129*, 292.
- Jia, Y.-X.; Zhong, J.; Zhu, S.-F.; Zhang, C.-M.; Zhou, Q.-L. *Angew. Chem., Int. Ed.* **2007**, *46*, 5565.
- Baudequin, C.; Zamfir, A.; Tsogoeva, S. B. *Chem. Commun.* **2008**, 4637.
- Terada, M.; Machioka, K.; Sorimachi, K. *Angew. Chem., Int. Ed.* **2006**, *45*, 2254.
- Zheng, W.; Wojtas, L.; Antilla, J. C. *Angew. Chem., Int. Ed.* **2010**, *49*, 6589.
- Uruguchi, D.; Sorimachi, K.; Terada, M. *J. Am. Chem. Soc.* **2005**, *127*, 9360.
- Holloway, C. A.; Muratore, M. E.; Storer, R. I.; Dixon, D. J. *Org. Lett.* **2010**, *12*, 4720.
- Kang, Q.; Zheng, X.-J.; You, S.-L. *Chem.—Eur. J.* **2008**, *14*, 3539.
- Kang, Q.; Zhao, Z.-A.; You, S.-L. *J. Am. Chem. Soc.* **2007**, *129*, 1484.

- (58) Guo, Q.-S.; Du, D.-M.; Xu, J. *Angew. Chem., Int. Ed.* **2008**, *47*, 759.
- (59) Rueping, M.; Antonchick, A. P. *Angew. Chem., Int. Ed.* **2007**, *46*, 4562.
- (60) Rueping, M.; Antonchick, A. P. *Angew. Chem., Int. Ed.* **2008**, *47*, 5836.
- (61) Schrader, W.; Handayani, P. P.; Zhou, J.; List, B. *Angew. Chem., Int. Ed.* **2009**, *48*, 1463.
- (62) Nguyen, T. B.; Bousserouel, H.; Wang, Q.; Guéritte, F. *Org. Lett.* **2010**, *12*, 4705.
- (63) Bachu, P.; Akiyama, T. *Chem. Commun.* **2010**, *46*, 4112.
- (64) Jiang, J.; Yu, J.; Sun, X.-X.; Rao, Q.-Q.; Gong, L.-Z. *Angew. Chem., Int. Ed.* **2008**, *47*, 2458.
- (65) Lu, M.; Lu, Y.; Zhu, D.; Zeng, X.; Li, X.; Zhong, G. *Angew. Chem., Int. Ed.* **2010**, *49*, 8588.
- (66) Xu, F.; Huang, D.; Han, C.; Shen, W.; Lin, X.; Wang, Y. *J. Org. Chem.* **2010**, *75*, 8677.
- (67) Simón, L.; Goodman, J. M. *J. Am. Chem. Soc.* **2008**, *130*, 8741.
- (68) Simón, L.; Goodman, J. M. *J. Org. Chem.* **2007**, *72*, 9656.
- (69) Chuma, A.; Horn, H. W.; Swope, W. C.; Pratt, R. C.; Zhang, L.; Lohmeijer, B. G. G.; Wade, C. G.; Waymouth, R. M.; Hedrick, J. L.; Rice, J. E. *J. Am. Chem. Soc.* **2008**, *130*, 6749.
- (70) Susperregui, N.; Delcroix, D.; Martin-Vaca, B.; Bourissou, D.; Maron, L. *J. Org. Chem.* **2010**, *75*, 6581.
- (71) Marcelli, T.; Hammar, P.; Himo, F. *Chem.—Eur. J.* **2008**, *14*, 8562.
- (72) Marcelli, T.; Hammar, P.; Himo, F. *Adv. Synth. Catal.* **2009**, *351*, 525.
- (73) Simón, L.; Goodman, J. M. *J. Am. Chem. Soc.* **2009**, *131*, 4070.
- (74) Simón, L.; Goodman, J. M. *J. Org. Chem.* **2009**, *75*, 589.
- (75) Shi, F.-Q.; Song, B.-A. *Org. Biomol. Chem.* **2009**, *7*, 1292.
- (76) Yamanaka, M.; Hirata, T. *J. Org. Chem.* **2009**, *74*, 3266.
- (77) Easson, L. H.; Stedman, E. J. *Biochem.* **1933**, *27*, 1257.
- (78) Vadim, A. D. *Chirality* **1997**, *9*, 99.
- (79) Gridnev, I. D.; Kouchi, M.; Sorimachi, K.; Terada, M. *Tetrahedron Lett.* **2007**, *48*, 497.
- (80) Simón, L.; Goodman, J. M. *J. Org. Chem.* **2010**, *75*, 589.
- (81) Liu, W.-J.; Chen, X.-H.; Gong, L.-Z. *Org. Lett.* **2008**, *10*, 5357.
- (82) Rueping, M.; Antonchick, A. P.; Brinkmann, C. *Angew. Chem., Int. Ed.* **2007**, *46*, 6903.
- (83) Xu, X.; Zhou, J.; Yang, L.; Hu, W. *Chem. Commun.* **2008**, 6564.
- (84) Yamanaka, M.; Itoh, J.; Fuchibe, K.; Akiyama, T. *J. Am. Chem. Soc.* **2007**, *129*, 6756.
- (85) Simón, L.; Goodman, J. M. *Org. Biomol. Chem.* **2011**, *9*, 689.
- (86) Goodman, J. M.; Silva, M. A. *Tetrahedron Lett.* **2003**, *44*, 8233.
- (87) Banik, B. K.; Lecea, B.; Arrieta, A.; de Cózar, A.; Cossío, F. P. *Angew. Chem., Int. Ed.* **2007**, *46*, 9347.
- (88) Tommaso Marcelli, F. H. *Eur. J. Org. Chem.* **2008**, *2008*, 4751.
- (89) Yu, J.; He, L.; Chen, X.-H.; Song, J.; Chen, W.-J.; Gong, L.-Z. *Org. Lett.* **2009**, *11*, 4946.
- (90) Akiyama, T.; Suzuki, T.; Mori, K. *Org. Lett.* **2009**, *11*, 2445.
- (91) Li, C.; Villa-Marcos, B.; Xiao, J. *J. Am. Chem. Soc.* **2009**, *131*, 6967.
- (92) Chen, X.-H.; Wei, Q.; Luo, S.-W.; Xiao, H.; Gong, L.-Z. *J. Am. Chem. Soc.* **2009**, *131*, 13819.
- (93) Wang, C.; Chen, X.-H.; Zhou, S.-M.; Gong, L.-Z. *Chem. Commun.* **2010**, *46*, 1275.
- (94) Rueping, M.; Antonchick, A. P. *Angew. Chem., Int. Ed.* **2008**, *47*, 10090.
- (95) Cheng, X.; Goddard, R.; Buth, G.; List, B. *Angew. Chem., Int. Ed.* **2008**, *47*, 5079.
- (96) Lifchits, O.; Reisinger, C. M.; List, B. *J. Am. Chem. Soc.* **2010**, *132*, 10227.
- (97) Wang, X.; List, B. *Angew. Chem., Int. Ed.* **2008**, *47*, 1119.
- (98) Traven, V. F.; Miroshnikov, V. S.; Pavlov, A. S.; Ivanov, I. V.; Panov, A. V.; Chibisova, T. y. A. *Mendeleev Commun.* **2007**, *17*, 88.
- (99) Berthet, J.; Delbaere, S.; Carvalho, L. M.; Vermeersch, G.; Coelho, P. J. *Tetrahedron Lett.* **2006**, *47*, 4903.
- (100) Steiner, T. *Angew. Chem., Int. Ed.* **2002**, *41*, 48.
- (101) Platts, J. A.; Howard, S. T.; Bracke, B. R. F. *J. Am. Chem. Soc.* **1996**, *118*, 2726.
- (102) Murray-Rust, P.; Glusker, J. P. *J. Am. Chem. Soc.* **1984**, *106*, 1018.
- (103) Taylor, R.; Kennard, O.; Versichel, W. *J. Am. Chem. Soc.* **1983**, *105*, 5761.
- (104) Hay, B. P.; Dixon, D. A.; Bryan, J. C.; Moyer, B. A. *J. Am. Chem. Soc.* **2002**, *124*, 182.
- (105) Simón, L.; Goodman, J. M. *J. Org. Chem.* **2010**, *75*, 1831.
- (106) Smith, S. G.; Goodman, J. M. *J. Am. Chem. Soc.* **2010**, *132*, 12946.